Surface Reactions of Molecular and Atomic Oxygen with Carbon Phosphide Films

ARTICLE *in* THE JOURNAL OF PHYSICAL CHEMISTRY B · NOVEMBER 2005

Impact Factor: 3.3 · DOI: 10.1021/jp0521196 · Source: PubMed

Surface Reactions of Molecular and Atomic Oxygen with Carbon Phosphide Films

Justin Gorham, Jessica Torres, Glenn Wolfe,† Alfred d'Agostino,‡ and D. Howard Fairbrother*

Department of Chemistry, Johns Hopkins University, 3400 North Charles Street, Baltimore, Maryland 21218

Received: April 23, 2005; In Final Form: August 22, 2005

The surface reactions of atomic and molecular oxygen with carbon phosphide films have been studied using X-ray photoelectron spectroscopy (XPS) and atomic force microscopy (AFM). Carbon phosphide films were produced by ion implantation of trimethylphosphine into polyethylene. Atmospheric oxidation of carbon phosphide films was dominated by phosphorus oxidation and generated a carbon-containing phosphate surface film. This oxidized surface layer acted as an effective diffusion barrier, limiting the depth of phosphorus oxidation within the carbon phosphide film to <3 nm. The effect of atomic oxygen (AO) exposure on this oxidized carbon phosphide layer was subsequently probed in situ using XPS. Initially AO exposure resulted in a loss of carbon atoms from the surface, but increased the surface concentration of phosphorus atoms as well as the degree of phosphorus oxidation. For more prolonged AO exposures, a highly oxidized phosphate surface layer formed that appeared to be inert toward further AO-mediated erosion. By utilizing phosphorus-containing hydrocarbon thin films, the phosphorus oxides produced during exposure to AO were found to desorb at temperatures >500 K under vacuum conditions. Results from this study suggest that carbon phosphide films can be used as AO-resistant surface coatings on polymers.

1. Introduction

The surface reactions of atomic oxygen (AO) are integral components of many plasma growth, etching, and decontamination processes.[1−3] The importance of AO is a reflection of its ability to oxidize organic films and carbonaceous surfaces to produce volatile, low-weight molecular species such as CO, CO_2, and H_2O.[4,5] In oxygen plasma sources employed for surface cleaning and decontamination, atomic oxygen (AO), predominantly in the ground $O(^3P)$ state, is often cited as the most important reactive species.[6,7] Similarly, the mass loss and erosion of polymer coatings used on spacecraft vehicles in low Earth orbit (LEO) has also been attributed to the oxidizing and etching properties of AO, specifically $O(^3P)$.[8−30] As a result, there has been interest in the development of organic coatings that can resist erosion in highly oxidizing environments. Such etch-resistant materials have potential as spacecraft coatings, oxygen plasma-resistant materials,[31] and as flame retardants.[32,33]

Phosphorus-containing polymers, such as polyphosphazenes and phosphine oxide-containing poly(arylene ethers), have been shown to exhibit improved resistance toward AO-mediated erosion.[34−38] For these phosphorus-containing polymers studies have proposed that, upon exposure to AO, selective etching of carbon from the surface produces a passivating phosphate overlayer that inhibits further erosion of the underlying polymer.[31,34,39] The detailed chemical and physical transformations that accompany the interaction of AO with phosphorus-containing polymers are, however, largely unexplored. To address this issue, carbon phosphide films, generated by ion implantation, were used in the present study as a model system to study the surface reactions of both atomic and molecular oxygen with a phosphorus-containing film. Because the resistance of any polymer toward AO is determined by the chemical characteristics of the surface, the present study is also motivated by the possibility that phosphorus ion implantation may offer an alternative strategy for generating AO-resistant coatings on a wide range of polymers.

Traditionally, phosphorus ion implantation has been achieved by using phosphine (PH_3).[40] The practical utility of phosphine is limited, however, by its toxicity. A recent study has shown that trimethylphosphine, $P(CH_3)_3$ (TMP), can also be employed as a source gas for phosphorus implantation.[41] On the basis of this study, we have employed TMP as a cheap, commercially available, and less hazardous source of phosphorus to generate carbon phosphide coatings on polyethylene. Because any surface coating generated by ion implantation under vacuum conditions will first be modified by atmospheric oxidation prior to AO exposure, the kinetics of phosphorus oxidation under atmospheric conditions as well as the structure and thickness of the phosphorus oxide overlayer that forms were also studied in this investigation. The subsequent reactions of oxidized carbon phosphide films with AO and the associated morphological changes were then studied in situ. Because surfaces exposed to AO can be modified significantly by atmospheric exposure,[42−44] these in situ surface studies are needed to develop a detailed understanding of the effect of AO exposure on phosphorus-containing materials. In related experiments, phosphorus-containing ultrathin hydrocarbon films have also been utilized to study the thermal stability of phosphorus oxides under vacuum conditions. Results from the present study indicate that ion implantation of trimethylphosphine can be used to generate AO-resistant coatings.

2. Experimental Section

Sample Preparation. Two different types of phosphorus-containing substrates were used in this investigation. In the majority of the experiments performed, carbon phosphide films

* Corresponding Author. E-mail: howardf@jhu.edu.
† Current Address: Department of Chemistry, University of Washington, Seattle, Washington.
‡ Department of Chemistry, College of Notre Dame, Maryland.

10.1021/jp0521196 CCC: $30.25
Published on Web 10/05/2005

generated on polyethylene (PE) substrates were studied. In these experiments, high-density polyethylene (HDPE) sheets (McMaster−Carr, technical grade) were cut into 1.5 cm × 1.5 cm squares and washed with ethanol, hexanes, and isooctane before being introduced into the ultrahigh vacuum (UHV) chamber through a fast-entry load lock. This cleaning procedure reduced oxygen impurities on the sample surface to less than 2% (as measured by XPS).

Preparation of Carbon Phosphide Films. Carbon phosphide films were generated on PE substrates by passing 20 mPa of TMP ($P(CH_3)_3$) vapor through a differentially pumped PHI 04-303 ion gun operating with 10 mA emission current and 4 kV acceleration voltage. TMP (Aldrich) was kept in a glass bulb attached to a gas manifold. TMP was purified by several freeze−pump−thaw cycles before the vapor was introduced into the ion gun through a UHV-compatible leak valve. Gas purity was routinely checked using mass spectrometry to verify the presence of the $P(CH_3)_3^+$ parent ion.[41] Following ion implantation, the surface became visibly discolored (darker).

Preparation of Phosphorus-Containing Ultrathin Hydrocarbon Films. Although the majority of studies reported in this investigation involved PE substrates modified by ion implantation with TMP, the thermal stability of phosphorus oxides under vacuum conditions was studied by synthesizing ultrathin (<5 nm) TMP-doped hydrocarbon thin films. These films were prepared on Au substrates that were mounted on dedicated UHV manipulators with facilities for sample cooling and heating. These ultrathin (<5 nm) films were generated by first dosing pentane (1×10^{-6} Torr for 45 min) onto a cooled (T < 130 K) gold substrate. Adsorbed pentane multilayers were then exposed to X-ray irradiation for 2 h. Secondary electrons generated by the incident X-rays initiated C−C and C−H bond breaking in the adsorbed film,[45] producing an ultrathin amorphous hydrocarbon film that remained stable at room temperature.[46,47] $P(CH_3)_3$ was then dosed on top of this amorphous hydrocarbon film at low temperatures (<130 K) and exposed to X-ray irradiation for several hours before the film was allowed to warm to room temperature. This approach produced ultrathin (<5 nm) phosphorus-containing amorphous hydrocarbon thin films.

Atmospheric Oxidation. The effect of air oxidation on carbon phosphide films was also studied. In these studies, samples were removed from the UHV chamber for controlled periods of time before being reintroduced into the vacuum chamber and analyzed with XPS.

Exposure to Atomic Oxygen (AO). Phosphorus-containing samples were exposed to AO using a thermal gas cracker TC-50 (Oxford Applied Research) positioned in a line-of-sight with the sample (target-to-sample distance of ≈ 5 cm).[20,21,48] The gas cracker operates by passing molecular oxygen through a metallic tube, which is heated to ≈ 1000 °C by electron beam irradiation. The heated capillary causes molecular oxygen to dissociate into a stream of atomic, low-energy AO in the ^3P state. Under these conditions, the AO species are assumed to have an average incident kinetic energy of $^3/_2\, kT_{capillary}$ (≈ 0.11 eV) during subsequent surface reactions. All of the experiments reported in this study were carried out with the AO source operating at 45 W and a chamber pressure of ≈ 6×10^{-7} Torr. One limitation of this thermal source is the deposition of small amounts of Ir on the surface after prolonged AO exposures; in the present study, the maximum surface concentration of Ir detected was ≈ 1% as measured by XPS.

X-ray Photoelectron Spectroscopy (XPS). In situ XPS analysis was carried out in a UHV chamber ($P_{base} \approx 5 \times 10^{-9}$ Torr) that contains both the AO source and the ion gun used for phosphorus ion implantation.[20,21,48] Because the modification of solid substrates by AO are dominated by reactions that occur at or in close proximity to the vacuum−film interface,[22] analytical methods such as XPS are particularly well suited for in situ investigations on the effect of AO exposure on organic films.[27,28]

XP spectra were acquired using a Mg Kα (1253.6 eV) X-ray source operating at 15 kV/300 W and a takeoff angle of 45° from the sample normal. All XP spectra in this study were acquired by using a hemispherical electron analyzer operating at a pass energy of 44.75 eV and a step size of 0.125 eV/step. XPS data were referenced to the C−C/C−H peak position at 284.6 eV. Except for the P(2p) region, XPS data analysis and peak fitting was performed with commercially available software using 100% Gaussian peaks and a Shirely background subtraction. Details of the experimental protocol used to fit the P(2p) region can be found in Section 3. Angle-resolved measurements were obtained by rotating the sample stage so that the takeoff angle between the sample normal and the electron analyzer varied between 10° (more bulk sensitive) and 80° (more surface sensitive).[49]

AFM Analysis. To examine changes in the surface topography during ion implantation and subsequent AO exposure, selected samples were examined with a PicoSPM LE AFM (Molecular Imaging) operating in magnetic AC tapping mode. Prior to imaging, samples were removed from the vacuum chamber via a fast-entry introduction chamber. All AFM images were taken ex situ by using silicon nitride cantilevers coated with a Co−Cr layer (MikroMasch). To identify the effects of AO exposure, carbon phosphide surfaces were imaged under ambient conditions before and after exposure to AO.

3. Results and Discussion

3.1. Formation and Characterization of Carbon Phosphide Films. Figure 1a shows the O(1s), C(1s), and P(2p) XPS regions following 60 min of phosphorus implantation into PE using TMP as a source gas. On the basis of analysis of the C(1s) and P(2p) XPS regions, the maximum P concentration produced under these ion implantation conditions (Ion Energy = 4 keV) ranged between 8 and 11%. The appearance of the peak in the P(2p) region centered at 131 eV (see Figure 1a) is indicative of the presence of C−*P* bonds.[38,50,51] After ion implantation of TMP, the surface is assumed to consist of an amorphous carbon phosphide film with some residual hydrogen in the form of C−H and P−H bonds.[50,51] Within this structure, phosphorus is bonded primarily through a network of C−P bonds,[51] as illustrated (schematically) in Figure 9. The asymmetry of the P(2p) peak (Figure 1a) was routinely observed after ion implantation. This phenomenon is believed to be a reflection of the chemical heterogeneity in the polymer surface induced by the ion implantation process; because of the lack of intensity in the O(1s) region, it cannot be attributed to the formation of oxidized phosphorus species. In the C(1s) region, the spectral envelope is attributed to a combination of *C*C/*C*H_2 and *C*−P bonded species whose binding energies are indistinguishable from one other.[38,50,51]

Angle-resolved XPS measurements (not shown) reveal that the P(2p):C(1s) area ratio is independent of the take-off angle, indicating that the extent of phosphorus implantation is uniform within the effective XPS analysis depth (≈ 5 nm).[52] After ion implantation with TMP, ex situ ATR analysis (Pike Technolgies MIRacle) revealed a loss of IR intensity in the vibrational modes

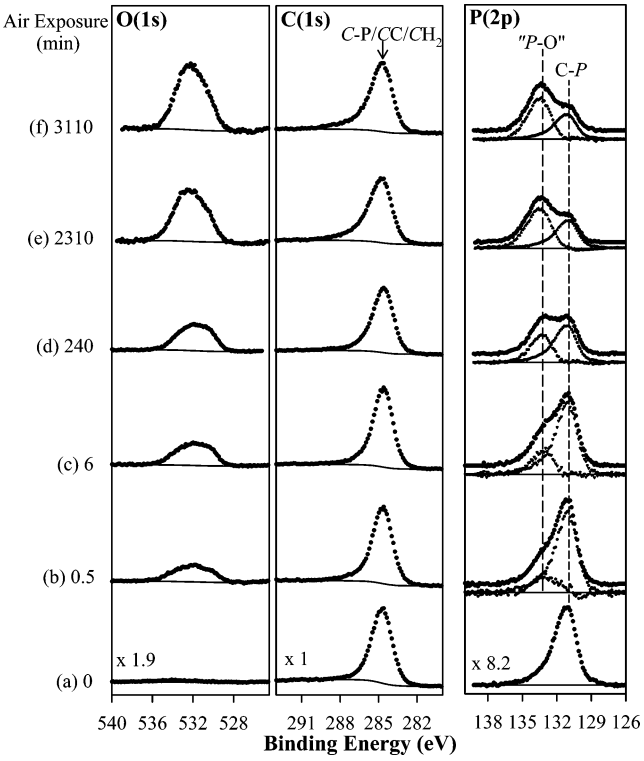

Figure 1. Variation in the O(1s), C(1s), and P(2p) XP spectral regions of carbon phosphide films after (a) 0, (b) 0.5, (c) 6, (d) 240, (e) 2310, and (f) 3110 min of atmospheric oxidation. Carbon phosphide films were generated by ion implantation using trimethyl phosphine (TMP). Raw data and fits are shown as solid circles (●) and backgrounds as solid lines (−). The experimental protocol used to generate the fits within the P(2p) XPS region is discussed in the text. The vertical dashed lines represent the peaks of the native C−P and "P−O" species centered at 131 and 133 eV, respectively.

associated with the CH_2 groups of the native PE substrate as well as the appearance of a new peak at ≈ 960 cm^{-1} (Figure 4). This new spectral feature is attributed to the formation of C−P bonds in the near-surface region as a result of the ion implantation process. The frequency of this band is lower than the C−P stretching frequency of TMP ($\upsilon_{C-P} = 1041$ cm^{-1}),[53] but higher than the C−P stretching frequencies in phosphorus carbides (computed to lie in the range 670−780 cm^{-1}).[54] Ex situ AFM analysis revealed that the formation of a carbon phosphide overlayer during ion implantation also increased the uniformity of the surface morphology compared to the native PE substrate and produced a modest increase in surface roughness (e.g., RMS 75 nm vs 68 nm).

3.2. Atmospheric Oxidation of Carbon Phosphide Films. The change in the O(1s), C(1s), and P(2p) spectral regions shown in Figure 1b−f reflect the evolution in the chemical composition of the carbon phosphide film as a function of atmospheric exposure time. Upon exposure of the carbon phosphide film to air (Figure 1b), spectral intensity is observed within the O(1s) region and grows with time. The O(1s) spectral envelope produced during air oxidation is broad (fwhm = 4 eV), indicating that the surface contains several different forms of oxidized species (e.g., P═O, C−O−P).[55] These observations are consistent with the idea that phosphorus oxidation is a result of reactions between C−P bonds and O_2/H_2O to form a mixture of PO_x species, such as P═O and P−OH. No detailed fitting of the O(1s) region was attempted, however, because of the overlap between different oxygen-containing species (e.g., P═O, P−O, C−O−P) with similar O(1s) binding energies.

XPS Fitting Protocol for the P(2p) Region. Atmospheric exposure also broadens the P(2p) region to higher binding energies, consistent with the formation of oxidized phosphorus species. Because of the distinct asymmetry of the native C−P peak (Figure 1a), spectral fitting of the overall P(2p) spectral envelope using either Gaussian or mixed Gaussian/Lorentzian functions proved unsatisfactory. The reactions of carbon phosphide films with oxygen produce oxidized phosphorus species whose P(2p) binding energies are shifted to higher binding energies than the native C−P species produced during the ion implantation process. Consequently, the XPS intensity contained within the low binding energy side of the P(2p) spectral envelope (between 131 and 129 eV) is assumed to be due exclusively to native C−P species. On the basis of this assumption, the spectral envelope associated with the oxidized phosphorus ("P−O") species was determined by subtracting the native C−P species from the overall P(2p) envelope. The relative contribution from the C−P and "P−O" species was determined by minimizing the difference between the raw data and the fitted spectra. Results of this analysis are shown in Figure 1. During the air oxidation process the position of the "P−O" peak remained nearly constant and centered at 133 eV, except for a slight shift (≈ 0.4 eV) to higher binding energies for prolonged atmospheric exposures (Figure 1).

In contrast to the pronounced changes within the P(2p) and O(1s) regions during air oxidation, the C(1s) region remains essentially unchanged (Figure 1b−d). For atmospheric exposures >2000 min (Figure 1e−f), however, the C(1s) peak did broaden slightly toward higher binding energies. On the basis of previous XPS measurements of phosphorus-containing flame retardants, this effect is ascribed to the formation of oxygen-containing carbon functionalities (e.g. *C*−O−P).[56] The broadening of the C(1s) region to higher binding energies could also result from the reactions between O_2 and carbon-containing radicals produced during ion bombardment. Reactions between oxygen and these surface radicals would, however, be expected to occur on a rapid time scale following exposure of the carbon phosphide film to air; this is inconsistent with the experimental data, where no change in the C(1s) spectral envelope is observed for all but the longest air exposures. Thus, the atmospheric oxidation of phosphorus-implanted PE, therefore, appears to be dominated by the oxidation of phosphorus. This assertion is also supported by a linear correlation between the "*P*−O" peak area in the P(2p) region and the overall integrated intensity within the O(1s) region (data not shown).

In Figure 1b−f, it is apparent that the rate of phosphorus oxidation decreases significantly for prolonged atmospheric exposures. Thus, even after 3110 min of atmospheric oxidation, native C−P species are still observed in the P(2p) region (Figure 1f). A more quantitative analysis of the phosphorus oxidation process is also possible on the basis of the fact that the attenuation of the P(2p) XPS peak area associated with the C−P species will decrease exponentially as the thickness of the oxidized carbon phosphonate (CPO_x) overlayer[49] (d) increases. Consequently, $\ln((C-P)_{t=0}/(C-P)_t)$ is directly proportional to the thickness of the oxidized carbon phosphonate overlayer. Analysis of Figure 2 indicates that the thickness of the oxidized phosphonate overlayer increases linearly with the natural log of total air exposure time (t). This type of behavior is indicative of a self-limiting reaction, where the diffusion of oxidizing species is kinetically hindered by the carbon-containing phosphate overlayer (CPO_x). On the basis of the linear regression shown in Figure 2, and an estimate of 3 nm for the inelastic mean free path of the P(2p) photoelectrons within the carbon

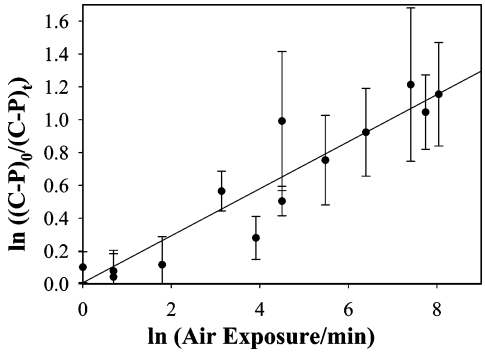

Figure 2. Variation in $\ln((C-P)_0/(C-P)_t)$ for a carbon phosphide film plotted as a function of the ln(atmospheric exposure time/min). $(C-P)_0$ and $(C-P)_t$ represent the integrated XPS area of the C−P species before and after air exposure for time t, respectively; $(C-P)_t$ was determined by peak fitting the P(2p) region. The solid line is a linear regression through the data and constrained to pass through the origin. Error bars have been computed on the basis of the uncertainty in determining the area of the $(C-P)_t$ species.

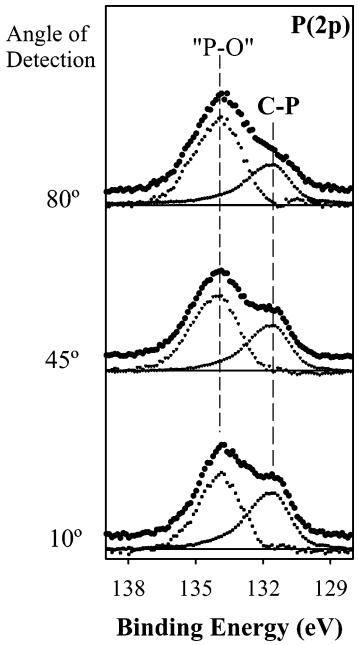

Figure 3. Angle-resolved XP spectra of the P(2p) region for a phosphorus-implanted PE surface exposed to air for 3110 min. Contributions from the native C−P species and the oxidized phosphorus ("P−O") species to the P(2p) envelope are shown. The detection angle is measured between the surface normal and the electron analyzer; therefore, the surface sensitivity of the XPS measurement increases on going from 10° to 80°.

phosphide film,[57,58] the thickness of the carbon-containing phosphate overlayer (d_{CPOx}) is given by the following expression:

$$d_{CPOx}\,(\text{Å}) = 2.8 \times \ln(\text{air exposure/min})$$

Thus, despite the thermodynamic driving force that exists for phosphorus oxidation, even after 3110 mins of air exposure, the thickness of the oxidized phosphorus overlayer is only ≈ 2.2 nm.

Angle-resolved P(2p) XP spectra of an air-oxidized carbon phosphide film, shown in Figure 3, indicate that the fraction of oxidized phosphorus species (higher binding energy peak) increases systematically as the take-off angle is varied from bulk sensitive (10°) to surface sensitive (80°) values. ATR analysis (Figure 4) also revealed that the intensity of the peak at ≈ 960 cm^{-1}, assigned to the C−P stretching frequency in the carbon phosphide film, remain virtually constant after >7 days of air exposure, and no new peaks associated with P═O or P−OH species are observed. Thus, XPS and ATR results both support the idea that phosphorus oxidation within the carbon phosphide overlayer is restricted to a depth of only a few nanometers; this is shown schematically in Figure 9.

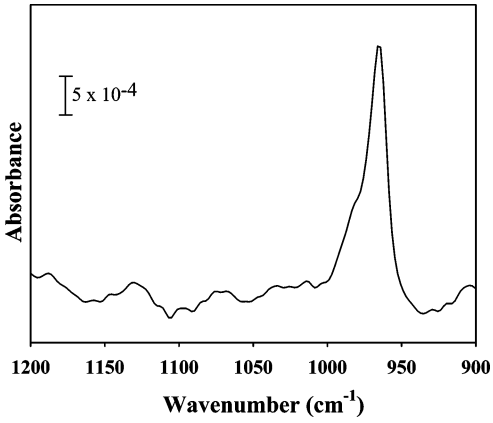

Figure 4. ATR−IR spectrum of PE after ion implantation with trimethylphosphine, showing the growth peak at ≈ 960 cm^{-1}. A loss of intensity associated with the CH_2 groups of the native PE was also observed during ion implantation.

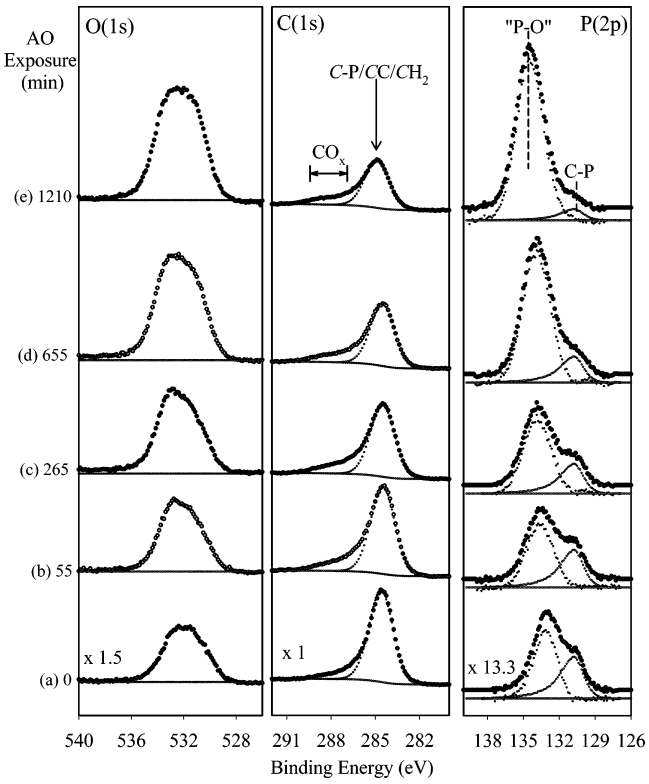

Figure 5. Effect of atomic oxygen (AO) exposure on the O(1s), C(1s), and P(2p) XP spectral regions of an air-oxidized carbon phosphide film. The experimental protocol used to generate the fits within the P(2p) XPS region for the C−P and "P−O" species is discussed in the text.

3.3. Effect of Atomic Oxygen Exposure on the Air-Oxidized Carbon Phosphide Films. The results presented in Figures 5−7 detail the impact of AO exposure on the surface of oxidized carbon phosphide films. Figure 5 illustrates the change in the C(1s), O(1s), and P(2p) spectral regions of the oxidized carbon phosphide overlayer (produced by atmospheric oxidation) as a function of AO exposure. Figure 6 shows the

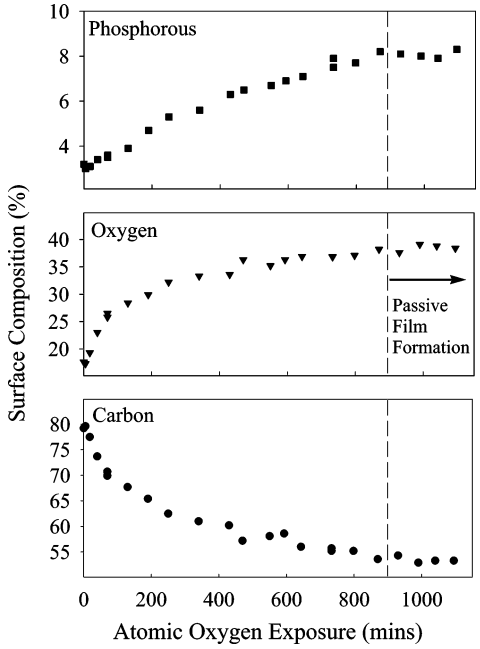

Figure 6. Variation in the integrated area of the C(1s), O(1s), and P(2p) XP peaks of an air-oxidized carbon phosphide film as a function of atomic oxygen (AO) exposure. The dotted line indicates the approximate AO exposure time required to produce a surface overlayer that remains invariant to further AO exposure.

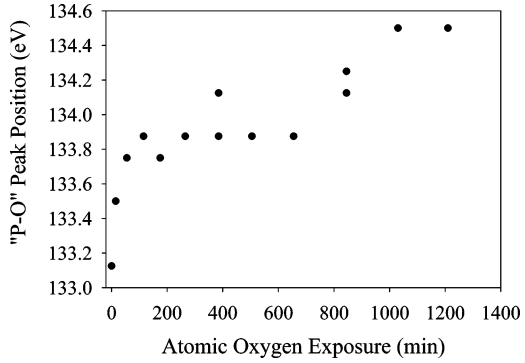

Figure 7. Variation in the "P−O" peak position (eV) as a function of AO exposure.

corresponding variation in the surface concentration of carbon, oxygen, and phosphorus, while Figure 7 shows the variation in the peak position of the oxidized phosphorus ("P−O") species as a function of AO exposure.

Prior to AO exposure, the C(1s), O(1s), and P(2p) XPS regions are consistent with the presence of an ultrathin, nanometer (<3 nm) thick carbon-containing phosphate surface layer, as discussed in Section 3.2. Figure 6 shows that exposing this overlayer to AO leads to a systematic decrease in the carbon content within the near-surface region. This decrease can be attributed to the etching of carbon through the formation of volatile, low-weight, carbon-containing species such as CO and CO_2.[59] In the C(1s) region of Figure 5, this is indicated by a decrease in the concentration of "hydrocarbon-like" ($C-C/CH_2$) carbon species. Despite the overall loss of carbon intensity, however, detailed analysis of the C(1s) region indicates that the concentration of oxidized carbon species (e.g., C−OH and COOH) initially increases as a result of AO exposure. This reflects the fact that oxidized carbon species (CO_x) such as alcohol and carboxylic acid groups are formed by the reaction of AO with CC/CH_2 species, analogous to the reactions of AO with alkanethiolate and carbonaceous thin films.[20,21] These CO_x moieties are, in fact, intermediates in the reaction between AO and hydrocarbon polymers,[20] thus,

$$C-H + AO \longrightarrow CO_{x(ads)}; \qquad CO_{x(ads)} + AO \longrightarrow CO/CO_2\uparrow$$

In contrast to the loss of carbon from the surface that accompanies AO exposure, analysis of the P(2p) region indicates that the phosphorus surface concentration increases steadily as a result of AO exposure (Figures 5 and 6). Enrichment of phosphorus at the surface occurs as a consequence of both the carbon etching that occurs during exposure of the film to AO and the resistance of the oxidized phosphorus species to AO-mediated erosion. More detailed analysis of the P(2p) spectral envelope (described in Section 3.3) reveals that the increase in the concentration of phosphorus at the surface during AO exposure is accompanied by: (i) a decrease in concentration of the C−P species and (ii) an increase in the integrated area of the "P−O" and the associated peak position from 133.1 to 134.6 eV (Figure 7). The decrease in concentration of C−P species in the near-surface region reflects the fact that increasing concentrations of phosphorus atoms are exposed to AO oxidation at the vacuum−film interface as carbon is selectively etched from the surface. Consequently, the increased phosphorus surface concentration is accompanied by a conversion of C−P species into oxidized "P−O" species.

The steady increase in the peak position of the "P−O" component with increasing AO exposure (Figure 5) indicates that AO exposure increases the average oxidation state of phosphorus atoms at the surface. This effect is a reflection of the greater oxidizing power of AO compared to O_2 as well as the range of effective oxidation states that phosphorus atoms can exhibit in different phosphorus oxides. Information on the nature of the oxidized phosphorus species contained within the "P−O" peak is best considered by measuring the difference in binding energy between the C−P and "P−O" peaks within the P(2p) region. Prior to AO exposure, the peak separation is ≈ 3 eV, consistent with the presence of $(RO)_3P{=}O$ bonds in alkyl phosphates.[60] Following 1200 min of AO exposure, the difference in binding energy between the C−P and "P−O" peaks increases to ≈ 4.7 eV (Figures 5 and 7); this is indicative of the presence of highly oxidized phosphate-type species that contain $O-P{=}O$ bonds (e.g. P_4O_6).[61] It should be noted that a similar increase in the P(2p) peak position has also been observed for phosphine oxide polymers exposed to oxygen plasmas.[31]

Despite the marked change in the chemical composition of the film during the initial period of AO exposure, analysis of Figures 5 and 6 indicates that, for AO exposures in excess of 800 min, the surface concentration of carbon, oxygen, and phosphorus remains constant. For these prolonged AO exposure times, the absence of continued enrichment in the P(2p) region, coupled with the constant O(1s) and C(1s) surface concentrations, implies the formation of a passivating surface layer that exhibits a greater etch resistance to AO. This is indicated in Figure 6 by a dotted line and is shown schematically in Figure 9.

The idea that the surface structure that forms after prolonged AO exposures exhibits increased resistance toward AO erosion is supported by studies carried out on the phosphorus-containing ultrathin (<5 nm) hydrocarbon films synthesized on Au substrates. In these experiments, exposure of AO produces a decrease in the intensity of the Au(4f) XPS peak. This finding is indicative of an increase in film thickness/density as a result of AO exposure and inconsistent with film erosion. In contrast, a monotonic increase in the Au(4f) XPS peak was observed when hydrocarbon films of similar thickness were exposed to

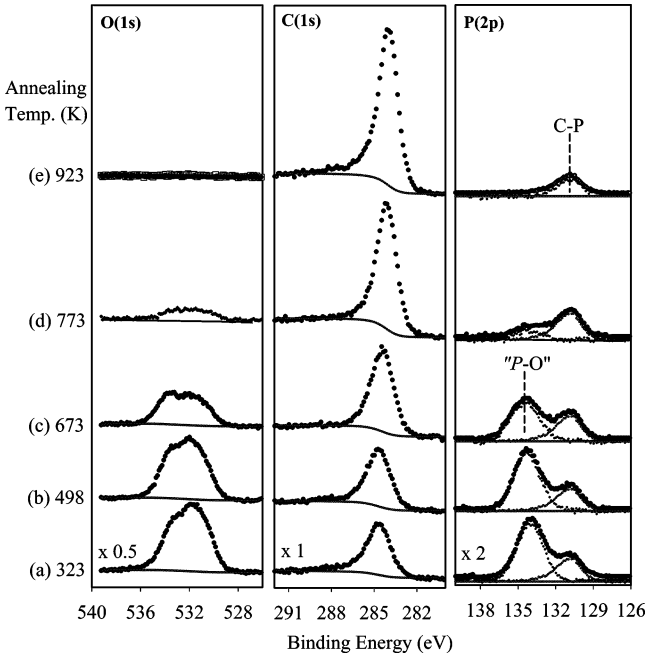

Figure 8. Variation in the O(1s), C(1s), and P(2p) XP spectral regions of an oxidized phosphorus-containing hydrocarbon films as a function of annealing temperature. In these experiments, ultrathin (<50 Å) phosphorus-containing films were grown on Au substrates. Details can be found in the Experimental Section.

AO, indicative of film erosion. These results, therefore, support the idea that the formation of a highly oxidized phosphorus layer that accompanies the reaction of AO with P-containing hydrocarbon films and polymers at the vacuum−film interface acts to retard AO-mediated erosion.

Results obtained in this investigation can also be compared to the effects of AO exposure on phenylphosphine oxide-containing polymers.[31,34,35,37−39,61] Figure 6 shows that, in the present investigation, following AO exposure, the surface of the oxidized carbon phosphide film is composed of 8% phosphorus, 39% oxygen, and 53% carbon. These values are very similar to the passivating surface layer that forms after poly(arylene ether phosphine oxide)s are exposed to an oxygen plasma treatment (10% phosphorus, 41% oxygen, and 46% carbon, as measured by XPS).[62] In the present study, the phosphate overlayer formed after prolonged AO exposure contains highly oxidized phosphorus species with a P(2p) binding energy of 134.6 eV (Figure 7). This value is similar to the P(2p) binding energy of ≈ 135.0 eV that has been observed previously for phosphorus-containing polymers exposed to AO in an oxygen plasma and also under LEO conditions.[31,34,62] Thus, it appears that the nature of the passivating phosphate overlayer produced in the present study is similar to the one produced when phosphorus-containing polymers such as poly(arylene ether phosphine oxide)s are exposed to AO. Indeed, results from the present investigation suggest that the formation of a protective surface layer during AO exposure is generic for different phosphorus-containing organic surfaces and polymers irrespective of how phosphorus atoms are incorporated into the near-surface region.

To probe the ability of carbon phosphide surface layers to function as protective coatings for spacecraft, further studies are needed under more realistic LEO conditions. This includes determining the effect of hyperthermal AO ($E_{kinetic}$ ≈ 5 eV) exposure rather than the thermal AO used in the present study. In addition, any synergistic effects involving AO and other reactive species such as VUV radiation, electrons, and charged particles that are also present in LEO would need to be identified. Results on the effects of LEO on phenylphosphine oxide-containing poly(arylene ether)s[39] have shown that carbon is etched from the surface and that the phosphorus concentration and level of oxidation increases during exposure to LEO. Weight loss data indicates that the phosphate layer that develops protects the underlying polymer from further erosion. O'Connell et al. have noted that these results are comparable to those obtained when the same polymers were exposed to lower kinetic energy AO (<1 eV) generated in an oxygen plasma. As a result, the similarities in the chemical composition of the passivating surface layer that forms after poly(arylene ether phosphine oxide)s are exposed to an oxygen plasma and the phosphate overlayer generated in our experiments suggests that carbon phosphide films will provide protection against hyperthermal AO in LEO.

In contrast to the pronounced chemical transformations that occur during AO exposure (Figures 5 and 6), AFM analysis reveals that the formation of the passivating phosphonate overlayer is not accompanied by any significant changes to the surface morphology. This is probably a reflection of the roughness of the initial carbon phosphide film formed by ion implantation, coupled with the fact that only a relatively small

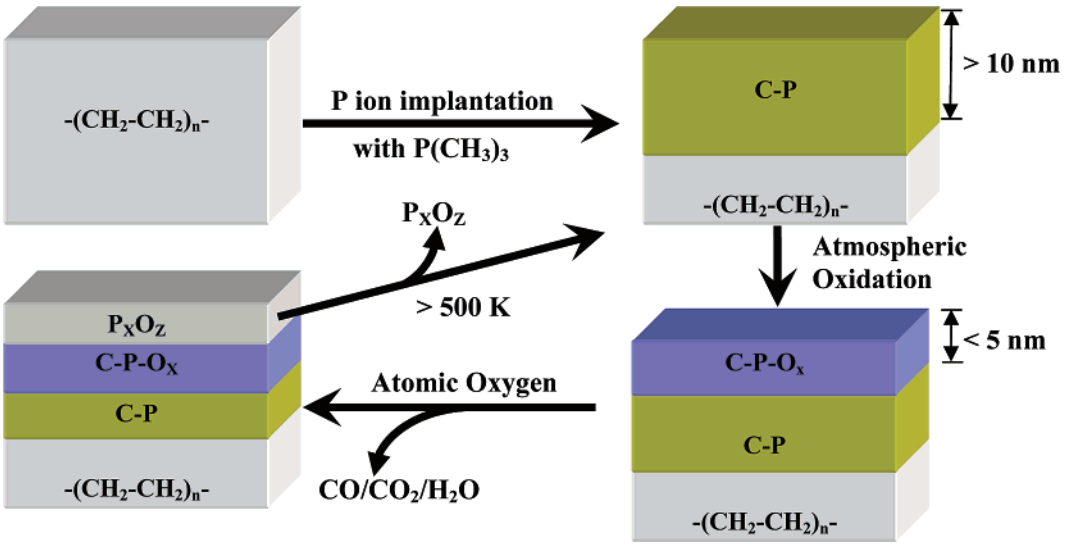

Figure 9. Schematic representation of the reactions of atomic and molecular oxygen with carbon phosphide films.

amount of AO-mediated erosion is necessary before the passivating phosphonate overlayer forms.

The thermal stability of the C−P and oxidized "P−O" species is shown in Figure 8. In these studies, ultrathin (<5 nm) oxidized carbon phosphide films were prepared on Au substrates, as described in the Experimental Section. Using this approach, the temperature of the film was varied by resistive heating and the thermal stability of the different phosphorus-containing species was identified by using XPS. A comparison of Figure 8a and b shows that the chemical composition of the surface remains constant below ≈ 500 K. Once a substrate temperature of 673 K is reached, however, XPS analysis reveals that the oxidized phosphorus ("P−O") species begin to desorb, presumably as volatile phosphorus oxides such as P_4O_{10}.[63] This is evidenced by a decrease in the "P−O" feature within the P(2p) region as well as a concomitant loss of intensity in the O(1s) region (Figure 8c); this is illustrated schematically in Figure 9. At 773 K, the oxidized phosphorus species have almost entirely desorbed; at 923 K, no oxidized phosphorus species remain in the film. In contrast, the carbon phosphide C−P species, formed during the initial ion implantation step, remain thermally stable at 773 K, although there is evidence of a decrease in the concentration of these species at temperatures >900 K. Figure 8 also illustrates that desorption of phosphorus and oxygen from the film produces a concomitant increase in the carbon concentration at the surface.

Although the principal focus of the principal investigation is to explore the surface reactions of molecular and atomic oxygen with carbon phosphide coatings and phosphorus-containing polymers, results from this study suggest that phosphorus ion implantation may offer a means to produce AO-resistant surface coatings on polymers. Indeed, ion implantation of carbon, boron, silicon, and aluminum has been used previously to generate AO-resistant layers on polymers.[59,64] One limitation of the self-passivating structure that forms during AO exposure, however, is the thermal stability of the resultant phosphorus oxides. Thus, on the basis of the results of this investigation, we anticipate that exposing carbon phosphide coatings or phosphorus-containing polymers to AO at high temperatures would lead to sustained erosion. Under these aggressive conditions, phosphorus oxide species will thermally desorb, while carbon is removed as volatile CO_2 and CO species. This synergistic effect of high temperatures and AO in terms of the stability of the carbon phosphide coating is illustrated by the closed loop within Figure 9. This has implications for the application of ion implantation as a means to generate protective coatings that require stability in higher-temperature situations (e.g., flame retardants).

4. Conclusions

The ion implantation of trimethylphosphine into polyethylene was used to produce amorphous carbon phosphide coatings on polyethylene; atmospheric oxidation of these films leads to the formation of a dense, nanometer-thick phosphate surface layer. Subsequent exposure of these films to atomic oxygen under vacuum conditions selectively etched carbon from the surface and enriched the surface concentration of phosphorus atoms until a highly oxidized phosphorus oxide structure formed at the vacuum−film interface. Experimental evidence suggests that this phosphorus-rich surface layer acted as a passivating film that can protect the underlying material from further AO-mediated erosion at substrate temperatures < 500 K. Results from the present investigation suggest that phosphorus ion implantation may be used to create AO-resistant coatings on a wide range of polymeric substrates.

Acknowledgment. Support for this research was provided by a National Science Foundation Career Award (no. 9985372) and a grant from the Petroleum Research Fund (PRF nos. 35281-G5, G6), administered through the American Chemical Society. Glenn Wolfe also acknowledges support from the Howard Hughes undergraduate research program administered through Johns Hopkins University. Professor Alfred d'Agostino also gratefully acknowledges support through the award of a Research Opportunity Award as a supplement to Professor Fairbrother's Career Award.

References and Notes

(1) Hsu, W. L. *J. Vac. Sci. Technol., A* **1989**, *7*, 1047.
(2) Herrmann, H. W.; Selwyn, G. S.; Henins, I.; Park, J.; Jeffery, M.; Williams, J. M. *IEEE Trans. Plasma Sci.* **2002**, *30*, 1460.
(3) Laroussi, M. *IEEE Trans. Plasma Sci.* **1996**, *30*, 1460.
(4) Bourdon, E. B. D.; Raveh, A.; Gujrathi, S. C.; Martinu, L. *J. Vac. Sci. Technol., A* **1993**, *11*, 2530.
(5) Ngo, T.; Snyder, E. J.; Tong, W. M.; Williams, R. S.; Anderson, M. S. *Surf. Sci.* **1994**, *314*, L817.
(6) Herrmann, H. W.; Henins, I.; Park, J.; Selwyn, G. S. *Phys. Plasmas* **1999**, *6*, 2284.
(7) Jeong, J. Y.; Babayan, S. E.; Tu, V. J.; Park, J.; Henins, I.; Hicks, R. F.; Selwyn, G. S. *Plasma Sources Sci. Technol*. **1998**, *7*, 282.
(8) Chambers, A. R.; Harris, I. L.; Roberts, G. T. *Mater. Lett.* **1996**, *26*, 121.
(9) Kleiman, J. I.; Gudimenko, Y. I.; Iskanderova, Z. A.; Tennyson, R. C.; Morison, W. D.; McIntyre, M. S.; Davidson, R. *Surf. Interface Anal.* **1995**, *23*, 335.
(10) Rasoul, F. A.; Hill, D. J. T.; George, G. A.; O'Donnell, J. H. *Polym. Adv. Technol.* **1998**, *9*, 24.
(11) Tennyson, R. C. *Can. J. Phys.* **1991**, *69*, 1190.
(12) Synowicki, R. A.; Hale, J. S.; Spady, B.; Reiser, M.; Nafis, S.; Woollam, J. A. *J. Spacecr. Rockets* **1995**, *32*, 97.
(13) Harris, I. L.; Chambers, A. R.; Roberts, G. T. *Mater. Lett.* **1997**, *31*, 321.
(14) Elms, F. E.; George, G. A. *Polym. Adv. Technol.* **1998**, *9*, 31.
(15) Nicholson, K. T.; Minton, T. K.; Sibener, S. J. *Prog. Org. Coat.* **2003**, *47*, 443.
(16) Minton, T. K.; Garton, D. J. *Dynamics of Atomic-Oxygen-Induced Polymer Degradation in Low Earth Orbit: Chemical Dynamics in Extreme Environments*; World Scientific: London, 2001; Vol. 11.
(17) Garton, D. J.; Minton, T. K.; Alagia, M.; Balucani, N.; Casavecchia, P.; Volpi, G. G. *Faraday Discuss.* **1997**, 387.
(18) Qin, X.; Tzvetkov, T.; Jacobs, D. C. *Nucl. Instrum. Methods Phys. Res., Sect. B* **2003**, *203*, 130.
(19) Zhang, J.; Garton, D. J.; Minton, T. K. *J. Chem. Phys.* **2002**, *117*, 6239.
(20) Torres, J.; Perry, C. C.; Bransfield, S. J.; Fairbrother, D. H. *J. Phys. Chem. B* **2002**, *106*, 6265.
(21) Wagner, A. J.; Wolfe, G. M.; Fairbrother, D. H. *J. Chem. Phys.* **2004**, *120*, 3799.
(22) Qin, X.; Tzvetkov, T.; Lee, D.-C.; Yu, L.; Jacobs, D. C. *J. Am. Chem. Soc.* **2004**, *126*, 13232.
(23) Troya, D.; Pascual, R. Z.; Garton, D. J.; Minton, T. K.; Schatz, G. J. *J. Phys. Chem. A* **2003**, *107*, 7161.
(24) Gindulyte, A.; Massa, L.; Banks, B. A.; Rutledge, S. K. *J. Phys. Chem. A* **2000**, *104*, 9976.
(25) Gindulyte, A.; Massa, L.; Banks, B. A.; Miller, S. K. R. *J. Phys. Chem. A* **2002**, *106*, 5463.
(26) Li, G.; Bosio, S. B. M.; Hase, W. L. *J. Mol. Struct.* **2000**, *556*, 43.
(27) Gonzalez, R. I.; Phillips, S. H.; Hoflund, G. B. *J. Appl. Polym. Sci.* **2004**, *92*, 1977.
(28) Hoflund, G. B.; Everett, M. L. *J. Phys. Chem. B.* **2004**, *108*, 15721.
(29) Everett, M. L.; Hoflund, G. B. *Macromolecules* **2004**, *37*, 6013.
(30) Hoflund, G. B.; Everett, M. L. *Appl. Surf. Sci.* **2005**, *239*, 367.
(31) Connell, J. W.; Smith, J. G.; Hedrick, J. L. *Polymer* **1995**, *36*, 13.
(32) Spirckel, M.; Reigner, N.; Mortaigne, B.; Youssef, B.; Bunel, C. *Polym. Degrad. Stab.* **2002**, *78*, 211.
(33) Morgan, A. B.; Tour, J. M. *J. Appl. Polym. Sci.* **1999**, *73*, 707.
(34) Smith, J. G.; Connell, J. W.; Hergenrother, P. M. *Polymer* **1994**, *35*, 2834.
(35) Connell, J. W. *High Perform. Polym.* **2000**, *12*, 43.
(36) Schuler, P.; Mojazza, H. B.; Haghighat, R. *High Perform. Polym.* **2000**, *12*, 113.
(37) Connell, J. W.; Smith, J. G.; Hergenrother, P. M. *Abstr. Pap. Am. Chem. Soc.* **1993**, *205*, 84.
(38) Watson, K. A.; Palmieri, F. L.; Connell, J. W. *Macromolecules* **2002**, *35*, 4968.

(39) Connell, J. W.; Smith, J. G.; Kalil, C. G.; Siochi, E. J. *Polym. Adv. Technol.* **1998**, *9*, 11.

(40) Kimm, K.-S.; Yang, M.-S.; Song, J.-K.; Hong, S.-H.; Kim, O. *Jpn. J. Appl. Phys., Part 1* **2004**, *43*, 6943.

(41) Oleszek, G. M. *J. Electrochem. Soc.* **2001**, *148*, 215.

(42) Grossman, E.; Lifshitz, Y.; Wolan, J. T.; Mount, C. K.; Hoflund, G. B. *J. Spacecr. Rockets* **1999**, *36*, 75.

(43) Wolan, J. T.; Hoflund, G. B. *J. Vac. Sci. Technol., A* **1999**, *17*, 662.

(44) Tagawa, M.; Yokota, K.; Omae, N.; Kinoshita, H. *J. Spacecr. Rockets* **2002**, *39*, 447.

(45) Wagner, A. J.; Carlo, S. R.; Vecitis, C.; Fairbrother, D. H. *Langmuir* **2002**, *18*, 1542.

(46) Wagner, A. J.; Han, K.; Vaught, A. L.; Fairbrother, D. H. *J. Phys. Chem. B* **2000**, *104*, 3291.

(47) Perry, C. C.; Wagner, A. J.; Fairbrother, D. H. *Chem. Phys.* **2002**, *280*, 111.

(48) Torres, J.; Wagner, A. J.; Perry, C. C.; Fairbrother, D. H. *Surf. Sci.* **2003**, *543*, 75.

(49) Vickerman, J. C. *Surface Analysis: The Principle Techniques*; John Wiley: New York, 1997.

(50) Pearce, S. R. J.; May, P. W.; Wild, R. K.; Hallam, K. R.; Heard, P. J. *Diamond Relat. Mater.* **2002**, *11*, 1041.

(51) Pearce, S. R. J.; Filik, J.; May, P. W.; Wild, R. K.; Hallam, K. R.; Heard, P. J. *Diamond Relat. Mater.* **2003**, *12*, 979.

(52) This value is based on the calculated inelastic mean free path of the C(1s) and P(2p) photoelectrons in polyethylene based on ref 57.

(53) O'Neill, J. A.; Passow, M. L.; Colter, T. J. *J. Vac. Sci. Technol., A* **1994**, *12*, 839.

(54) Claeyssens, F.; Fuge, G. M.; Allen, N. L.; May, P. W.; Ashfold, M. N. R. *J. Chem. Soc. Dalton Trans.* **2004**, *19*, 3085.

(55) Rebeyrat, S.; Grosseau-Poussard, J. L.; Silvain, J. F.; Panicaud, B.; Dinhut, J. F. *Appl. Surf. Sci.* **2002**, *199*, 11.

(56) Qu, B.; Xie, R. *Polym. Int.* **2003**, *52*, 1415.

(57) Orosz, G. T.; Gergely, G.; Menyhard, M.; Toth, J.; Varga, D.; Lesiak, B.; Jablonski, A. *Surf. Sci.* **2004**, *566*−*568*, 544.

(58) This value is estimated from the inelastic mean free path of P(2p) photoelectrons in polyethylene (ref 57).

(59) Iskanderova, Z.; Kleinman, J.; Guidimenko, Y.; Morrison, W. D.; Tennyson, R. C. *Nucl. Instrum. Methods Phys. Res., Sect. B* **1997**, *127*/*128*, 702.

(60) Sodhi, R. N.; Cavell, R. G. *J. Electron. Spectrosc. Relat. Phenom.* **1983**, *32*, 283.

(61) Lee, T. H.; Jolly, W. L.; Bakke, A. A.; Weis, R.; Verkade, J. G. *J. Am. Chem. Soc.* **1980**, *102*, 2631.

(62) Smith, C. D.; Grubbs, H.; Webster, H. F.; Gungor, A.; Wightman, J. P. *High Perform. Polym.* **1991**, *3*, 211.

(63) Muenow, D. W.; Uy, O. M.; Margrave, J. L. *J. Inorg. Nucl. Chem.* **1970**, *32*, 3459.

(64) Lee, E. H.; Lewis, M. B.; Blau, P. J.; Mansur, L. K. *J. Mater. Res.* **1991**, *6*, 610.